Predicting vertical concentration profiles in the marine atmospheric boundary layer with a Markov chain random walk model

Hyungwon John Park[1], Thomas Sherman[1,4], Livia S. Freire[2], Guiquan Wang[1], Diogo Bolster[1], Jeffrey S. Reid[3], and David H. Richter[1]

[1]University of Notre Dame, Notre Dame, Indiana, USA.
[2]University of São Paulo, São Carlos, Brazil.
[3]U.S. Naval Research Laboratory, Monterey, California, USA.
[4]FTS International, LLC, Dulles, Virginia, USA.

Key Points:

- A proof of concept is proposed for predicting vertical distribution of aerosol particles
- A large eddy simulation (LES) model is used to train a Markov chain random walk model in the cloud-free marine atmospheric boundary layer
- The random walk model can replicate LES statistical outputs for a wide range of particle sizes and varying atmospheric stabilities

Corresponding author: H. J. Park, Hpark6@nd.edu

Abstract

In an effort to better represent aerosol transport in meso- and global-scale models, large eddy simulations (LES) from the NCAR Turbulence with Particles (NTLP) code are used to develop a Markov chain random walk model that predicts aerosol particle vertical profiles in a cloud-free marine atmospheric boundary layer (MABL). The evolution of vertical concentration profiles are simulated for a range of aerosol particle sizes and in a neutral and an unstable boundary layer. For the neutral boundary layer we find, based on the LES statistics, that there exist temporal correlation structures for particle positions, meaning that over short time intervals ($T = 500\,\mathrm{s}$, or $T/T_{\mathrm{neut}} = 0.25$), particles near the bottom of the boundary are more likely to remain near the bottom of the boundary layer than being abruptly transported to the top, and vice versa. For the unstable boundary layer, a similar time interval of $T = 500\,\mathrm{s}$ ($T/T_{\mathrm{eddy}} = 0.39$) exhibits weaker temporal correlation compared to the neutral case due to the strong non-local convective motions. In the limit of a large time interval, $T = 2000\,\mathrm{s}$ ($T/T_{\mathrm{eddy}} = 1.56$), particles have been mixed throughout the MABL and virtually no correlation exists. We leverage this information to parameterize a Markov chain random walk model that accurately predicts the evolution of vertical concentration profiles for the range of particle size and stability tested in LES, even over short time intervals which exhibit substantial correlation. The new methodology has significant potential to be applied at the subgrid level for coarser-scale weather and climate models.

1 Introduction

At the ocean surface, the combination of winds and breaking waves generate sea spray aerosol droplets that are transported throughout the marine atmospheric boundary layer (MABL) (Andreas, 1998; de Leeuw et al., 2000; Veron, 2015). Suspended in the atmosphere, sea spray aerosol particles can act as cloud condensation nuclei (Ghan et al., 1998; Lewis & Schwartz, 2004; Clarke et al., 2006), influence the propagation of electromagnetic radiation (Stolaki et al., 2015; Gerber, 1991), and interact with geochemical cycles of reactant species (Erickson et al., 1999). The impact on these processes depends on the aerosol number concentration, mass loading, chemical composition, and sea spray aerosol particle diameter, which spans a wide distribution (Reid et al., 2008; Quinn et al., 2015). To address these influences, observational and model-based studies have investigated the vertical distribution of sea spray aerosol particles in the atmosphere (Reid et al., 2001; Bian et al., 2019).

To study the influence of turbulence on aerosol particle transport processes, high fidelity numerical simulations of the MABL can be used. In particular, large eddy simulations (LES) have been used to understand the dynamics of boundary layers (Moeng, 1984), characterize their statistical turbulence properties (Deardorff, 1972), and investigate plume dispersion (Lamb, 1978; Wyngaard & Brost, 1984). Upscaling the governing physical processes with bulk parameters is of interest due to the large computational cost associated with explicitly resolving the wide distribution of length and time scales in the MABL. In environmental fluid flows, the ratio between the largest and smallest length scales of motion can span more than six orders of magnitude. To alleviate the cost of attempting to resolve all scales, modelers use coarse grid resolutions; global aerosol models as well as meso-scale systems have grid lengths between one and hundreds of kilometers (Riemer et al., 2003; Christensen et al., 2003). Consequently, large scale models then neglect small scale processes, but it is imperative to provide coarse-scale models with accurate representations of subgrid distributions of aerosol particle concentrations. This representation is particularly important along the sea surface, where aerosol particles are generated and are mostly confined (Blanchard et al., 1984; Toba, 1965).

One approach for parameterizing the turbulent transport of sea spray aerosol particles in the MABL has been through the use of one-dimensional column models (Rouse,

1937; Prandtl, 1981; Kind, 1992; Hoppel et al., 2002). These models attempt to describe vertical concentration profiles taking into account gravitational settling as well as net surface emission, and have been extended to account for a range of atmospheric stabilities (Chamecki et al., 2007; Freire et al., 2016). These studies rely on Monin-Obukhov similarity theory to predict aerosol concentration profiles in the surface layer, while Nissanka et al. (2018) extended this to capture profiles for the full MABL. While providing reasonable predictions in the case of neutral stability, in the case of unstable atmospheric stability, expressing turbulent fluxes by the gradient diffusion hypothesis (also known as first-order K-theory) limits the accuracy of the prediction of vertical concentration profiles (Stull, 1988) and so a different approach is needed. Here we propose such an alternative approach, aimed at providing both rapid and accurate predictions of aerosol concentrations for varying size and stability suitable as a basis for parameterizations in global and perhaps mesoscale aerosol models.

To do this, we upscale transport using a correlated random walk framework. Random walks are commonplace, ranging across applications including financial markets (Scalas, 2006; Montero & Masoliver, 2017), electron transport (Nelson, 1999), animal foraging patterns (Giuggioli et al., 2009), and solute transport in hydro-geologic systems (Le Borgne et al., 2008; Berkowitz et al., 2006). Particle trajectories through space and time are modeled as a series of stochastic jumps (i.e., random walk), most commonly sampled as independent identically distributed. In this study however, we adopt a correlated random walk model that is conceptually similar to that applied in the subsurface hydrology community (Le Borgne et al., 2008; De Anna et al., 2013; Bolster et al., 2014), although we apply correlation in time, while in hydrogeology correlation in spatial jumps arises more frequently. The key assumption in a correlated random walk model is that a particle's transport behavior at every model step is dependent not only on its current state, but also on its history. The correlated random walk model we propose has a one step memory, where a particle's current transition depends on its last.

We apply this random walk framework to model the evolution of a constant surface source of aerosol particles in the MABL. Aerosol particle mass is discretized into many point particles that transition through time and space by sampling a probability distribution that governs particle motion. Specifically, we model a particle's vertical position through time. By considering many particle trajectories, our upscaled framework predicts the vertical transport of aerosol particles through a cloud-free MABL, allowing effective modeling of the temporal evolution of vertical concentration profiles. Similar upscaled transport models in the context of hydrologic systems have displayed computational costs 6 orders of magnitude less than high fidelity simulations (e.g. Sherman et al. (2019)), meaning that transport behavior can be faithfully predicted at future times without resolving the turbulent flow field. Though the focus of this study is geared toward sea spray aerosol particles over the open ocean, this modeling strategy can in principle be applied to anthropogenic, dust, or any other kind of particle over various landscapes. In this study, we test the robustness of our method by considering both neutral and unstable boundary layers and for a range of aerosol particle sizes. Although the model is trained on known, idealized LES simulations, the proposed modeling framework here is used as a proof of concept study to offer a step toward an accurate, computationally efficient aerosol particle transport model.

2 Numerical Methodology

2.1 Large eddy simulations

This study uses the National Center for Atmospheric Research (NCAR) LES model in which the Eulerian fields of mass, momentum and energy are solved from the filtered

Navier-Stokes equations under the Boussinesq approximation:

$$\frac{\partial \tilde{u}_i}{\partial x_i} = 0, \tag{1}$$

$$\frac{\partial \tilde{u}_i}{\partial t} = -\frac{\partial \tilde{u}_i \tilde{u}_j}{\partial x_j} - \frac{\partial \tau_{ij}}{\partial x_j} + \frac{g\delta_{i3}}{T_0}\tilde{\theta} - \frac{1}{\rho_0}\frac{\partial \tilde{p}}{\partial x_i} + f(\tilde{u}_2 - V_g)\delta_{i1} + f(U_g - \tilde{u}_1)\delta_{i2}, \tag{2}$$

$$\frac{\partial \tilde{\theta}}{\partial t} = -\tilde{u_i}\frac{\partial \tilde{\theta}}{\partial x_i} - \frac{\partial \tau_{\theta i}}{\partial x_i}, \tag{3}$$

where $\tilde{u}_i$ is the resolved velocity, $\tilde{\theta}$ is the resolved potential temperature, $\tilde{p}$ is the resolved pressure, τ_{ij} is the subgrid stress, f is the Coriolis parameter, and $\tau_{\theta i}$ is the subgrid turbulent flux of potential temperature. The Eulerian subgrid-scale turbulent fluxes are parameterized by the model proposed by Deardorff (1980). We assume the large-scale pressure gradient balances the Coriolis force by imposing a constant geostrophic wind speed, U_g.

The flow is driven by this geostrophic wind, in which only one direction is considered ($U_g = 10\,\mathrm{m/s}, V_g = 0$). The Eulerian representation of the carrier phase is assumed periodic in the horizontal (x and y) directions and resolved on a uniform grid in all Cartesian directions. An inversion layer is imposed at the upper half of the domain's vertical extent, in addition to a radiation condition at the top of the domain (Klemp & Durran, 1983). A pseudo-spectral discretization is used for spatial gradients in the horizontal directions, whereas a second-order finite difference scheme is used in the vertical direction. Time integration is done with a third-order Runge-Kutta method, and a divergence-free filtered velocity field is enforced via a fractional step method. The lower boundary conditions are prescribed by the rough-wall Monin-Obukhov similarity relations, and the surface is assumed flat with a constant aerodynamic roughness (0.001m). The base LES code (without Lagrangian point-particles) has been used previously in many studies of the planetary boundary layer (Moeng, 1984; Sullivan & Patton, 2011).

Sea spray aerosol particles are represented as Lagrangian point-particles, which are assumed smaller than the smallest scales of turbulence (Balachandar & Eaton, 2010). Particle motion follows a Langevin equation:

$$x_{p,i}(t + \Delta t) = x_{p,i}(t) + v_{p,i}\Delta t + \eta_i\sqrt{2K(x_{p,i})\Delta t} + \frac{d\overline{K}(x_{p,3})}{dz}\Delta t\delta_{i3}, \tag{4}$$

$$v_{p,i} = u_{f,i} - \tau_p g\delta_{i3}, \tag{5}$$

where the velocity of the particle ($v_{p,i}$) is dictated by the local resolved fluid velocity ($u_{f,i}$), which is retrieved at the location of the particle using 6th order Lagrange interpolation. It is further modulated by the settling velocity $\tau_p g$, where $\tau_p = \rho_p d_p^2/18\rho_f\nu_f$ is the Stokes time scale for a sphere (Brennen, 2005). In equation 4, η_i is an independent and identically distributed random value from a normal distribution. The sub-grid diffusivity $K(x_{p,i})$ describes the turbulent dispersion of the Lagrangian particle; it is obtained from the LES sub-grid eddy diffusivity (for a passive scalar) interpolated to the particle location. Overbars refer to averaging in the horizontal directions. The fourth term, $d_z\overline{K}(x_{p,3})\Delta t$, takes into account vertical transport that is caused by spatial variations in mean diffusivities and conserves mass-balance that would otherwise be violated (see (Delay et al., 2005), equation 40 for more details).

For our particular simulation setups, the domain size and number of grid points are held fixed at $1500 \times 1500 \times 850\,\mathrm{m}$ ($x \times y \times z$) and $128 \times 128 \times 128$, respectively. The timestep is set to 0.5 seconds with an initial temperature inversion of $0.50\,\mathrm{K/m}$ at approximately 570 m. The use of the strong inversion is to maintain approximately steady state conditions with minimal boundary layer growth. We consider aerosol particle sizes with diameters of 2, 10, and 50 μm to test the influence of gravitational settling on transport behavior and particle aerosol lifetime.

Two simulations without particles are performed to allow the turbulent flow field to fully develop and reach steady state conditions. The first one corresponds to 3 hours with neutral atmospheric stability, whereas the second run is for 1 hour with unstable stratification. The same geostrophic wind ($U_g = 10\,\mathrm{m/s}$) is imposed on both neutral and unstable cases. For the unstable case, a surface heat flux of $0.02\,\mathrm{K\text{-}m/s}$ is used. In relation to meteorological conditions, this corresponds to a air-sea temperature difference of roughly $1.5°$ C. Once the flow field fully develops, particles are generated randomly along an $x - y$ plane at the first vertical gridpoint ($z = 3.12\,\mathrm{m}$); 100 particles are initialized at each LES time step (200 particles per second). The source flux is denoted as $\phi_s = 200\,s^{-1}$. If the Lagrangian particles are transported below the lower surface ($x_{p,3} \leq 0$), the particle is removed from the simulation, representing dry deposition.

LES, like all models, makes explicit assumptions and is only valid when those assumptions are reasonable. In the LES considered here, the simulated Lagrangian sea spray aerosol particles maintain a constant size, meaning that hygroscopicity and aerosol swell are not considered (Winkler, 1988). The changing atmospheric conditions due to the diurnal cycle have been neglected, as have momentum and energy exchange between the aerosol particles and the air (e.g. neglecting the effects of spray modifying heat and moisture in the surface layer (Peng & Richter, 2019)). Lastly, the LES assumes a flat surface with a prescribed aerodynamic roughness length, although in the open ocean the moving surface waves may play a substantial role in the transport and fate of sea spray aerosol particles (Richter et al., 2019).

2.2 Markov chain random walk model

Particle transport behavior simulated in the LES is used to develop the upscaled random walk model. As an initial proof of concept, we consider only the vertical transport of aerosol particles, where a full 3-D representation can be developed in future studies. In the Markov chain random walk framework, particles transition through time and space by sampling a probabilistic distribution for spatial and temporal jumps $\phi(x, t)$. A particle's trajectory is conceptualized as series of jumps, where each jump has an associated distance and time; this is the conceptual basis of a random walk model. Here we fix time, meaning each jump occurs over a constant model time step T, but the associated travel distance varies. Then, under the assumption of independent spatial and temporal jumps we can write $\phi(x, t) = \psi(x)\delta(t - T)$. Physically, the sampled travel distance represents the net vertical displacement of a particle over the given lapsed time T.

With this we can describe particle motion with the Langevin equation

$$\begin{aligned} t_i^{n+1} &= t_i^n + T \\ z_i^{n+1} &= z_i^n + \ell^{n+1}, \quad \ell \in \psi(\ell^{n+1}|\ell^n) \end{aligned} \tag{6}$$

At every model step, particle i travels a net distance ℓ over model time step T. The vertical displacement ℓ at every model step is sampled from a global distribution $\psi(\ell)$. Since a particle's vertical displacement in T is conditioned by its position in the atmospheric column, we sample ℓ from a conditional distribution, meaning that a particle's position at the next model step depends on its current position. Particle trajectories are therefore conceptualized as a Markov chain with their position at the next model step only depending on their current position. In this Markov chain random walk framework, particle trajectories are conditionally sampled via a transition matrix, which gives the probability that a particle transitions from its current height to any other z location in the boundary layer after model time step T.

Successive model jumps may be independent (or decorrelated), meaning that a particle's predicted vertical position after an interval T is independent of its initial position.

If independence is assumed throughout the vertical extent, then the Markov chain is not necessary and a randomly sampled location would suffice. Therefore, we note that the random walk framework describes the overall model, which may or may not take account into correlation via the Markov chain and transition matrix M. Over shorter timescales T, it is necessary to take into consideration this correlation; i.e., particles at the bottom (or top) of the boundary layer are more likely to stay at the bottom (or top) of the boundary layer. This correlation structure is what necessitates the use of the Markov chain component of the random walk model.

2.2.1 Vertical position correlation structure: transition matrix

In the Markov chain model, particles transition through space according to the probabilistic rules of a transition matrix M. Again, the transition matrix describes probabilities that a particle changes from one location to another in a fixed time. Conceptually, we discretize the atmospheric boundary layer into S height bins, with bins 1 and S representing the lowest and highest vertical positions in the boundary layer, respectively. This discretization represents the global distribution $\psi(l)$ into M. Matrix M then has size $[S, S]$ and each element in $M_{i,j}$ is the probability that a particle trajectory after a T ends in bin j given in started in bin i; i.e.,

$$M_{i,j} = P(z^{n+1} \in \text{ bin } j | z^n \in \text{ bin } i). \tag{7}$$

By definition, this requires that the summation of any row in M is unity. The Markov chain model contains the critical assumption of temporal stationarity of the transport processes, meaning that the transition matrix elements for any T window are identical. One of the benefits of this transition matrix approach is that it can model nonlocal behaviors (i.e. particles can jump large distances in the domain and are not just restricted to communicate with adjacent cells).

In the LES, detailed statistics gathered from a large number of individual Lagrangian particle trajectories are used to construct M. Specifically, we run a steady-state LES simulation over a time T (Eqn. 6) and track many ($O(10^6)$) particles to estimate each element of M. The particles begin uniformly dispersed throughout the boundary layer height, meaning that each starting bin is weighted equally. A separate LES calculation is performed for each aerosol particle size to construct the size-dependent transition matrices.

The total simulation time required to run the LES consists of: the time for the LES to develop steady-state turbulence, and then an additional time T to compute the transition matrix M as well as the injection distribution ψ_I (explained later) of the random walk model. The goal is to only need to run the LES for a time T, from which the upscaled model can make predictions out to much later times. In this study, the boundary layer is partitioned into 20 bins of equal size; i.e., each bin has height of approximately 15 m. With full knowledge of M and an initial particle location, we can effectively model a particle's vertical position through time and therefore predict the evolution of vertical aerosol particle concentration profiles.

2.2.2 Boundary condition: removal of particles

Aerosol particles that reach the ocean surface by dry deposition ($x_{p,3} < 0$) in the LES are removed from the simulation. Such behavior must therefore also be faithfully captured within the Markov chain random walk model. To do so, we add an additional bin to M, representing transport to the ocean surface. If a particle transitions to this surface bin, the particle is removed from the system. In the context of stochastic models this is often called transport to a limbo state (Van Kampen, 1979; Sund et al., 2015). Parameterization of this "limbo" bin is consistent with the methods discussed above; i.e., in the LES we track the number of particles that transition from height z to the surface

after T, and this is included in the transition matrix M as an additional column. In the results section, the choice of T is shown to influence the probabilities of dry deposition.

2.2.3 Initial condition: particle injection $\psi_I(z)$

For the MABL system considered here, sea spray aerosol particles are continuously emitted from the ocean surface into the atmospheric boundary layer. This means that under certain conditions, namely when the number of aerosol particles injected into the atmosphere exceeds the number of aerosol particles depositing onto the ocean surface, the total aerosol particle number will increase through time. We parameterize this behavior in the Markov chain random walk model by adding a distribution of aerosol particles at every model step. This distribution corresponds to the vertical distribution of any new particles generated over the last T seconds. We first numerically calculate ψ_I from LES statistics; ψ_I is simply the vertical concentration profile of particles released during a window of time T. Additionally, we demonstrate that in neutral conditions, ψ_I can be parameterized from existing one-dimensional models, potentially removing the need to calculate ψ_I from LES. In this study, we assume that the ψ_I distribution is stationary for any interval $[t, t+T]$, though ψ_I varies slightly across various intervals for unstable cases. In the LES we add 200 particles per second to the domain, and therefore $200T$ for a random walk model time step. Note that the actual injected number is slightly less than $200T$ because some particles are emitted and absorbed back into the ocean within the model time step T; i.e. the lifetime of a particle is permitted to be less than T.

3 Results

Here we briefly summarize the parameterization of the Markov chain random walk model after statistically steady-state turbulence is achieved. Using LES, we empirically find the two upscaled model input parameters: M and ψ_I. This is done for each atmospheric condition/particle diameter combination. In this section, we first characterize the neutrally stratified boundary layer and use the LES particle statistics for the comparison and validation of the upscaled model. Afterwards, we perform the same procedure for an unstably stratified boundary layer.

3.1 Neutral boundary layer

Once aerosol particles are generated at the surface, the vertical transport mechanisms affecting their displacement are the local turbulence and the settling effect of gravity. If the strength of settling is less than that of the vertical velocity seen by the Lagrangian particles throughout their lifetime, then they have a high probability of reaching the top of the boundary layer. If particles are too heavy, they have a high likelihood of quickly falling back into the ocean. In the case of neutral boundary layers, the wind shear is solely responsible for the mechanical generation of turbulence. Therefore, characterizing the turbulent kinetic energy (or specifically the vertical velocity variance) is useful in understanding vertical transport of sea spray aerosol particles. Neutral boundary layers as an atmospheric state can be used as a helpful model development testbed and as a proxy for other conditions (Stull, 1988).

3.1.1 Characterization of the neutral boundary layer

For the neutral case, Figure 1 presents snapshots of LES vertical velocity, with horizontal planes at two heights: 100m and 300m, corresponding to $z/z_i = 0.18$ and $z/z_i = 0.53$, where z_i is the boundary layer height. Near the surface, coherent structures of vertical velocities are smaller than near the middle of the boundary layer (300m), where larger-scale coherent turbulent structures are more visibly apparent. In Figure 1(c), the nor-

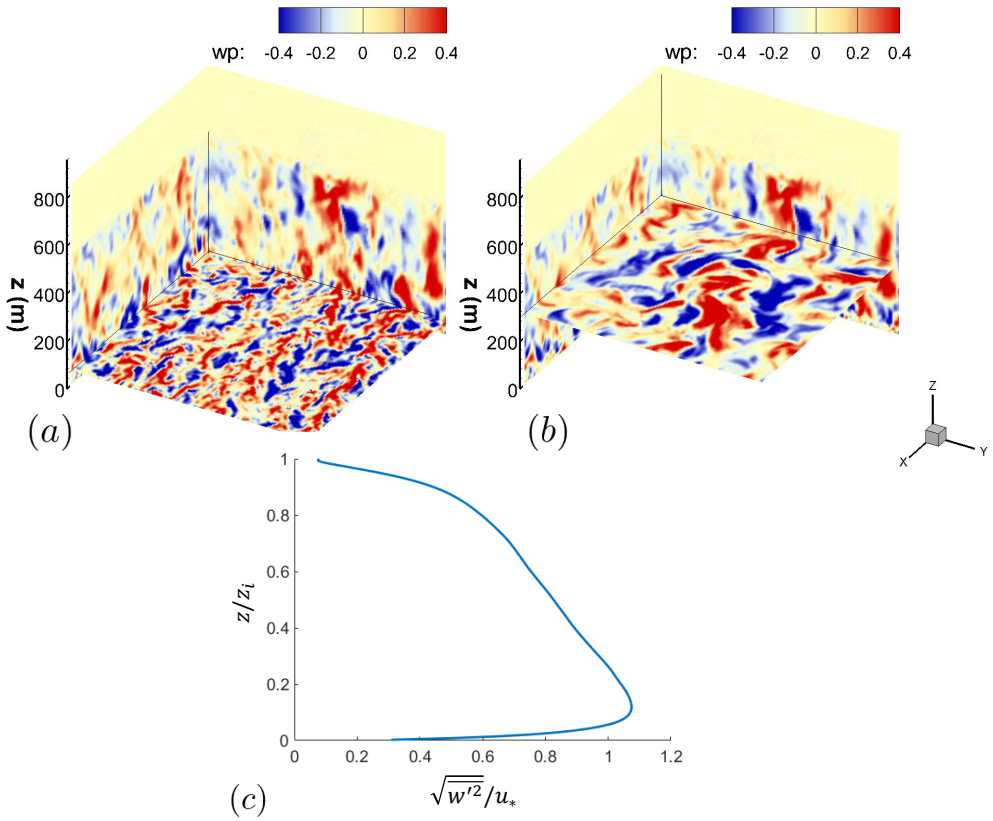

Figure 1. Snapshot of instantaneous vertical velocity with an horizontal planes at (a) 100m ($z/z_i = 0.18$) and (b) 300m ($z/z_i = 0.53$) for the neutral boundary layer. (c) is the time-averaged vertical profile of root-mean-squared vertical velocity normalized by u_*, the friction velocity.

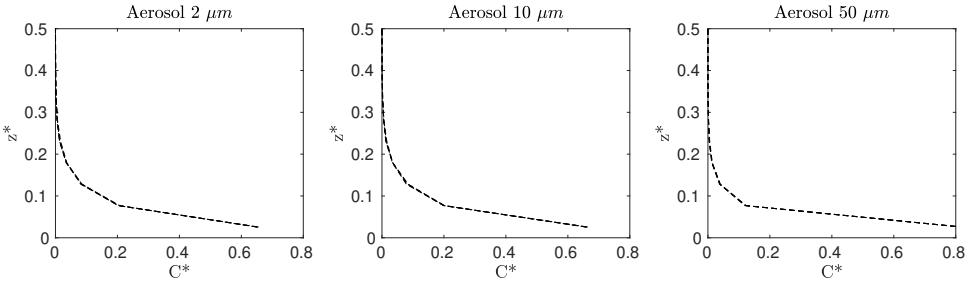

Figure 2. The distribution of newly generated aerosol particles ψ_I in a $T/T_{\text{neut}} = 0.25$ window for neutral conditions. The y-axis is the normalized vertical height $z^* = z/z_i$, and the x-axis is the normalized concentration $C^* = C(z)/C_T$, where $C(z)$ is the concentration of particles at a bin location, and C_T is the total concentration for a given snapshot. 20 different temporal snapshots of ψ_I are shown in each panel (but overlap).

malized root-mean-square of the vertical velocity exhibits a peak near the surface, in accordance with other studies (Deardorff, 1972). This quantity can be interpreted as a measure of the turbulence intensity experienced by the aerosol particles.

The vertical concentration profile of newly generated sea spray aerosol particles (over time T) is measured in the LES to parameterize ψ_I. For neutral stability, the value of T is normalized by the neutral stratification time scale $T_{\text{neut}} = z_i/u_*$ (u_* is the friction velocity), which is around 2000 seconds. We choose the normalized model time step $T/T_{\text{neut}} = 0.25$ (where $T = 500\,\text{s}$), which is sufficiently large such that the transition matrix displays temporal stationarity, but small enough such that a Markov chain is required to capture correlations between particle jumps. Figure 2 shows the vertical concentration profiles for $T/T_{\text{neut}} = 0.25$ generated for 20 different windows $[nT, (n+1)T]$ for particles with diameter 2, 10, and 50 μm. This profile reflects the distribution ψ_I of the newly injected particles in the upscaled model. Note that we have plotted all 20 distinct profiles for each aerosol particle diameter, but they are all nearly identical and hence appear as a single profile. This overlap indicates that the turbulence is statistically steady-state based on the chosen T. For all aerosol particle sizes, the majority of newly generated particles remains in the lower atmosphere, meaning that $T/T_{\text{neut}} = 0.25$ is not sufficiently long for particles to sample the entire boundary layer. Again, this correlation is what necessitates the use of a Markov chain component of the random walk model.

As the diameter increases, the gravitational settling velocity increases, causing a higher concentration of particles near the surface as observed in Figure 2. Physically, larger particles require persistent and strong updrafts to reach the upper portions of the boundary layer, whereas smaller particles are more likely to reach greater heights and stay suspended without the need of constant upward velocities. Thus, larger particles exhibit lower concentrations as vertical height increases.

3.1.2 Markov chain random walk prediction

We apply the Markov chain random walk model to predict aerosol particle transport through the boundary layer and compare model predictions with the LES. Using the Lagrangian statistics, the transition matrix is parameterized, as shown in the top panels of Figure 3. The position of an aerosol particle based on the normalized model time step $T/T_{\text{neut}} = 0.25$ is strongly correlated to its current position. Such behavior is captured by the transition matrices, which display strong diagonal trending; i.e. particles

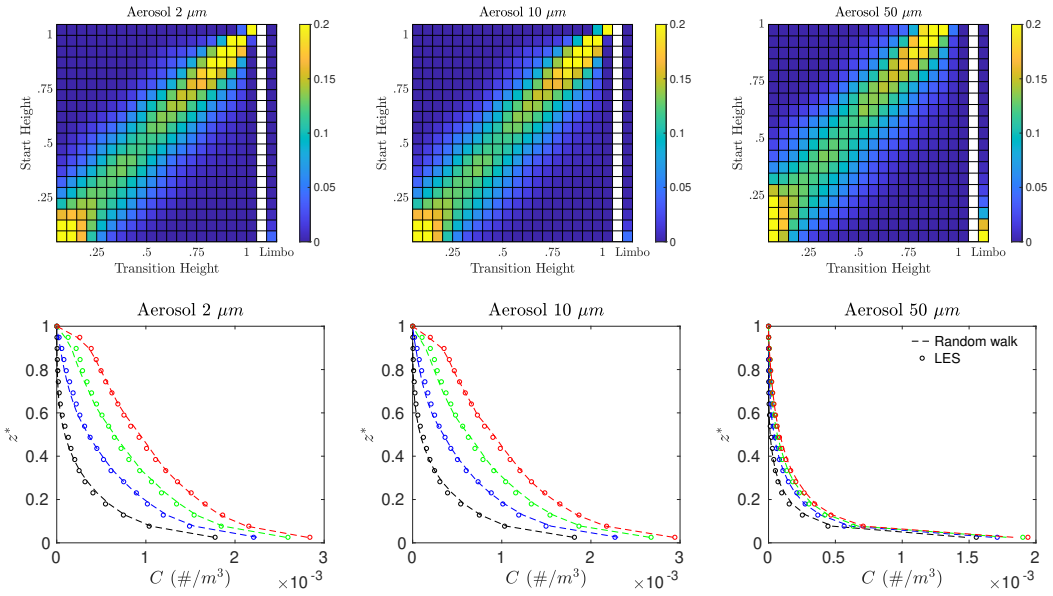

Figure 3. The top row is the transition matrices for particles with diameter $d = 2, 10, 50\,\mu$m with a normalized model time step $T/T_{\text{neut}} = 0.25$, where $T = 500\,$s. The bottom row is the temporal evolution of the vertical aerosol particle concentration profiles in the neutral boundary layer for LES (dots) and the Markov chain upscaled model predictions (dashed line). Colors correspond to $t/T_{\text{neut}} = 1$ (black), 2 (blue), 3 (green) and 4 (red), where t is the time since the first sourcing of particles. Concentrations are provided as a local number density based on the number of particles in the LES.

that start at the bottom (or top) of the boundary layer are likely to stay at the bottom (or top).

For dry deposition to the surface, the rightmost column of the transition matrices quantifies the transition from some height to the ocean. As the distance between the ocean surface and current particle position decreases, the probability that the particle enters limbo (dry deposition) increases. Furthermore, as the particle's diameter increases its probability of removal increases, seen as increased values in the removal column of the transition matrices — an effect well-captured by the transition matrix and upscaled model.

Using this parameterization, the Markov chain model accurately represents the LES evolution of vertical concentration for 2, 10, and 50 μm diameter particles. Figure 3 shows the horizontally-averaged concentration profile at snapshots of $t/T_{\text{neut}} = 1$ (black), 2 (blue), 3 (green) and 4 (red) along the bottom row of panels. As a reference, the reported concentrations are the number concentration from the LES given the injection rate ($\phi_s = 200\,s^{-1}$). The atmosphere begins devoid of particles, and over time the particle concentration increases as they are continuously injected at $z = 0$. As time evolves, particles have sufficient time to sample the full range of motions in the boundary layer, and turbulent dispersion results in the transport of particles throughout the boundary layer. For the $d = 2, 10\,\mu$m cases, turbulence is strong enough for such transport; however in contrast, very few particles with a diameter of 50 μm make it to the top of the boundary layer because the turbulent field is too weak in comparison to gravitational settling. These features are well-captured by the upscaled model.

3.2 Unstable (convective) boundary layer

We now consider an unstable boundary layer in addition to the neutral conditions of the previous section. The surface heat flux in this scenario corresponds to a 1.5° C air sea temperature difference, a typical setting over open oceans. In addition to the imposed geostrophic wind, buoyancy production of convective turbulence occurs due to the relatively warm surface. The significant amount of vertical mixing due to these convective motions causes a near-constant concentration with height, a feature in the profile which is very difficult for traditional 1-D analytical models to capture (Nissanka et al. (2018), hereafter referred to as N18).

3.2.1 Characterization of unstable boundary layer

Figure 4 presents snapshots of vertical velocity with planes at two different heights, as well as a profile of vertical velocity fluctuations. Note that compared to Figure 1, the scales for vertical velocity fluctuation are up to three times larger. In the wall-normal $x-y$ planes, convective plumes are visible via large, coherent regions of vertical velocity fluctuation. These large scale features are important to the transport of aerosol particles, as it will be shown to significantly affect the positional correlation structures in the transition matrix. Additionally, the normalized root-mean-square of the vertical velocity shows the maximum of vertical mixing toward the center of the mixed layer, in agreement with other studies (Moeng & Sullivan, 1994).

We use the standard definition of the convective velocity scale $w_* = [g z_i (\overline{w'\theta'})_s / T_s]^{1/3}$ to define a convective large eddy time-scale, $T_{\text{eddy}} = z_i / w_*$. Here, T_s is the reference surface temperature (273 K), $\overline{w'\theta'}$ is the surface heat flux, and g is gravitational acceleration. Our convective time scale is roughly 20 minutes, consistent with previous studies (Moeng & Sullivan, 1994). We first choose a model time step of $T = 500\,\text{s}$, which corresponds to $T/T_{\text{eddy}} = 0.39$. By choosing T less than T_{eddy}, the model time interval will be less than the time required to mix aerosols throughout the MABL, thus necessitating the Markov chain. It will be shown that even in this case, the upscaled transport model can reasonably predict near-vertical concentration profiles in the mixed layer. Additionally, we anticipate that using a normalized model time step $T/T_{\text{eddy}} > 1$ leads to particle decorrelation, removing the necessity of a Markov chain since particles would have time to sample the entire MABL. Therefore, we also test a case when T is larger than T_{eddy}: $T = 2000\,\text{s}$, or $T/T_{\text{eddy}} = 1.56$.

Figure 5 displays ψ_I for both $T/T_{\text{eddy}} = 0.39$ (top rows) and $T/T_{\text{eddy}} = 1.56$ (bottom rows). Each panel contains multiple profiles, representing different simulation windows of the corresponding normalized model time steps T. Due to our simulation times ending at t=11400s, the model time step $T = 2000\,\text{s}$ allows for 5 unique instances of ψ_I. In the neutral case, all ψ_I are nearly identical, however under unstable conditions we observe that the profile of newly generated aerosol particles is somewhat variable in time. We attribute this variation to the large scale turbulent structures, which influence the convergence of time-averaged statistics. At the surface layer and inversion layer heights, the initial injection distributions are similar, where the large scale structures are less dominant.

As expected, $T/T_{\text{eddy}} = 0.39$ displays concentrations that are able to reach the upper half of the boundary layer, unlike the neutral ψ_I. Particle concentration is the largest in the surface layer, because aerosols are generated at the surface and are carried downwards by gravity – again this becomes stronger with particle size. We choose the first profile, i.e., the vertical concentration profile at $t = T$, as the injection initial condition ψ_I for both values of T. For the case with $T = 2000\,\text{s}$, the profile ψ_I looks similar to the fully-developed concentration profile, as expected since the particles have had sufficient time to distribute and sample the entire MABL.

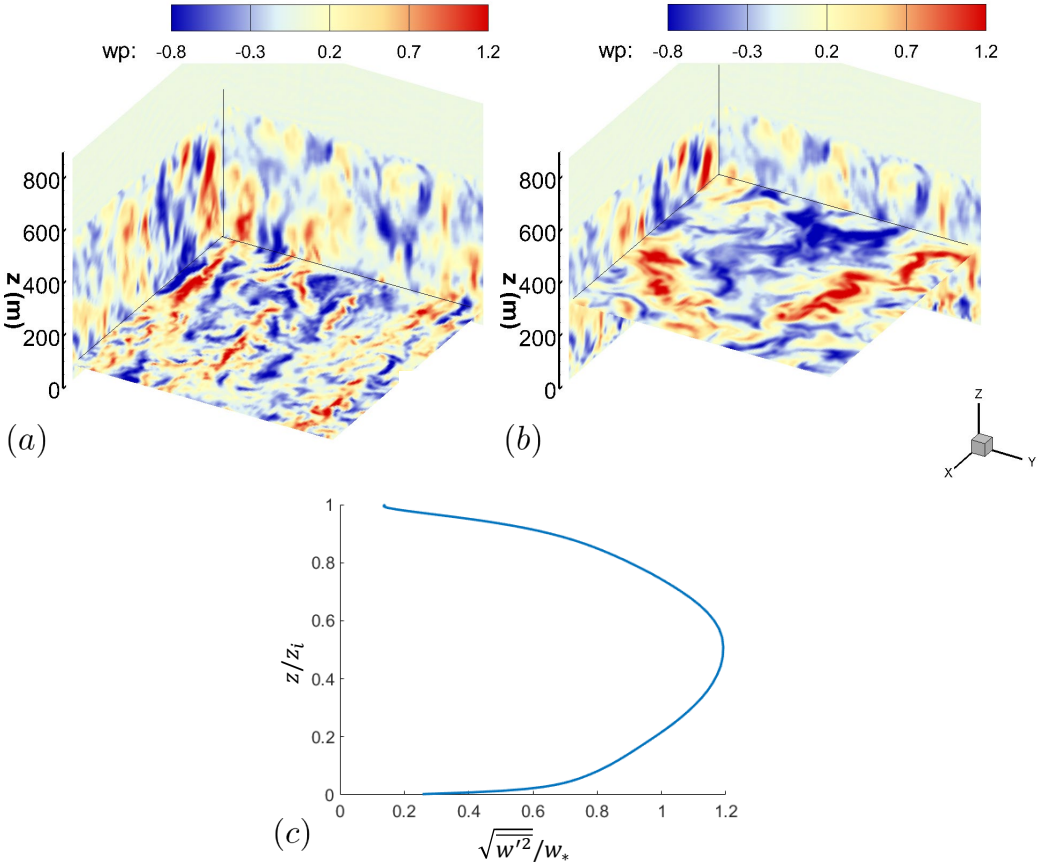

Figure 4. Snapshot of instantaneous vertical velocity with horizontal planes at (a) 100 m ($z/z_i = 0.18$) and (b) 300 m ($z/z_i = 0.53$) for the unstable boundary layer. (c) the time-averaged vertical profile of root-mean-squared vertical velocity normalized by the convective velocity scale.

3.2.2 Markov chain random walk

We apply the same methodology of using the LES to determine M and ψ_I to parameterize the upscaled model. In this section we present two random walk simulations using the two values of T for the unstable boundary layer, and note the difference in vertical concentration predictions.

For unstable stratification, the transition matrix when using $T/T_{\text{eddy}} = 0.39$ is shown in the top row of Figure 6, and exhibits generally weaker correlation throughout the mixed layer as compared to the neutral boundary layer (top rows of Figure 3). Particle correlations are greater toward the surface and the inversion layer, where particles tend to remain for successive time intervals.

When using these transition matrices, the bottom rows of Figure 6 compare the model predictions to the LES results. Above a height of $z/z_i \approx 0.2$, the random walk model correctly predicts a near-uniform concentration profile, due to the enhanced vertical mixing relative to the neutral boundary layer. As noted above, it is this feature which is very difficult for traditional eddy diffusivity models to capture. As the concentration of aerosols grows in the boundary layer, the Markov chain random walk model generally exhibits an underprediction within the surface layer. Compared to the neutral case shown in Figure 3, there is more variation in the predictions for the unstable case, which

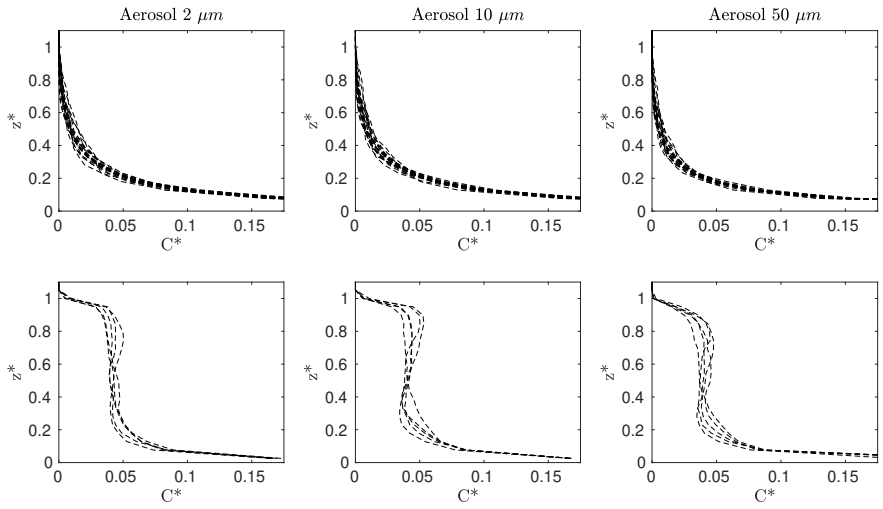

Figure 5. The distribution of newly generated aerosol particles ψ_I in for two model time steps T under unstable conditions. The concentration is normalized in the same way as the neutral condition. 20 unique temporal snapshots of ψ_I are shown for $T = 500$, while 5 are shown for $T = 2000$, demonstrating the temporal variability of the initial condition.

is consistent with that seen in the profiles of ψ_I and reflects the time variability of the horizontally averaged concentration. Similarly, the transition matrix at multiple instances of $T/T_{\text{eddy}} = 0.39$ undergoes slight temporal variation (not shown), but the general features remain the same since the flow is statistically stationary.

When setting $T/T_{\text{eddy}} = 1.56$ ($T = 2000\,\text{s}$), the transition matrices reflect the well-mixed behavior exhibited in the concentration profiles, displayed in the top panels of Figure 7. As expected, the matrices are nearly uniform, meaning that a particle's initial position is not correlated to the particle's final position since the model time step T is larger than the convective time scale. We again observe that increasing the aerosol particle size increases the probability that a particle enters limbo within the interval T, and the probability of particle limbo is larger in the selection of $T/T_{\text{eddy}} = 1.56$ than in $T/T_{\text{eddy}} = 0.39$.

When using $T/T_{eddy} = 1.56$, for all particle sizes the random walk model accurately captures the evolution of mean aerosol concentration; this is shown in the bottom panels of Figure 7. As mentioned above, $T/T_{\text{eddy}} = 1.56$ now takes into account the largest convective time-scale. Once considering this time-scale, the Markov chain nearly completely decorrelates (within the surface and mixed layer), eliminating the need of a Markov chain and transition matrix formulation. Effectively, the injection initial condition of the random walk (ψ_I) contains all of the information needed to make predictions, since it captures the shape of the well-mixed concentration profile.

4 Discussion

With the results of the vertical concentration profile predictions for all considered particle sizes and stabilities, we can now expand upon analysis of the Markov chain random walk model. As mentioned before, the random walk model currently requires M and ψ_I, which are obtained from the LES. With the goal of reducing computational cost associated with running LES, we begin this discussion by inferring new transition matrices based on already-calculated transition matrices — i.e., from several matrices M

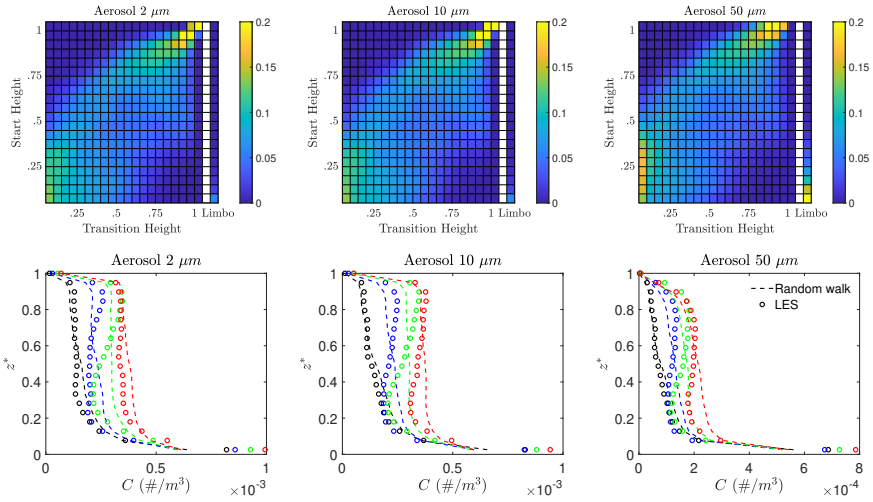

Figure 6. Transition matrices are shown above for particles with diameter $d = 2, 10, 50\,\mu$m using the normalized model time step $T/T_{\text{eddy}} = 0.39$, where $T = 500\,$s. The bottom panels are the temporal evolution of the vertical aerosol particle concentration profiles in the unstable boundary layer for LES (dots) and Markov chain upscaled model predictions (dashed lines). The random walk concentration is the scaled concentration with respect to the LES (see section 3.1.2). Colors correspond to $t/T_{\text{eddy}} = 0.39$ (black), 0.78 (blue), 1.17 (green) and 1.56 (red).

calculated from LES of a limited set of particle sizes, M for other particle sizes can be predicted without needing additional LES.

With an eye on removing the need for using LES at all, we also discuss the possibility of using 1-D theory on particle distribution to specify ψ_I, and discuss the sensitivity of the model predictions to M in order to assess how robust the predictions of C would be to various (future) parameterizations of M.

4.1 Inference of M based on particle size

So far we have shown predictions for models that were parameterized from the LES directly, meaning that we have full access to highly detailed Lagrangian trajectory data. However, such parameterization methods still require LES (albeit for much shorter durations) and therefore demands potentially large computational resources. In other words, we still need to simulate transport in order to predict transport, which somewhat defeats the purpose of upscaled modeling. In this section we use the previously calculated transition matrix data to infer how the transition matrix changes with aerosol particle size. Doing so means we can parameterize random walk models for a large range of particle sizes by gathering statistics from just a few LES cases, thereby reducing the computational costs associated with the parameterization step.

To demonstrate, we infer the transition matrix of a particle with diameter 35 μm from the transition matrices observed for particles with diameters 2, 5, 10, 20, 50 μm for the unstable and neutral boundary layers. To do so requires an adjustment of the probability of each transition matrix element with respect to particle size. Anticipating that the elements of the transition matrix scale with particle mass based on gravitational settling, thus depending on d_p^3, we find a least-squares best fit polynomial of degree 3; this reflects that the transition matrix elements are a function of particle volume. We find

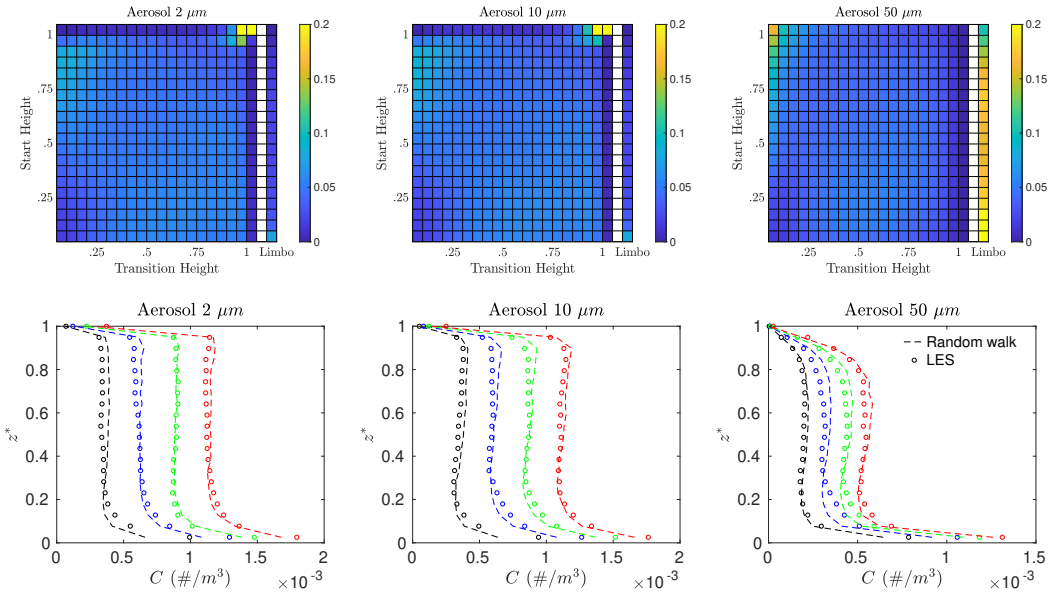

Figure 7. Transition matrices are shown below for particles with diameter $d = 2, 10, 50 \mu m$ using the normalized model time step $T/T_{\text{eddy}} = 1.56$, where $T = 2000s$. The bottom panels are the temporal evolution of the vertical aerosol particle concentration profiles in the unstable boundary layer for LES (dots) and Markov chain upscaled model predictions (dashed line). Colors correspond to $t/T_{\text{eddy}} = 1.56$ (black), $t/T_{\text{eddy}} = 3.13$ (blue), $t/T_{\text{eddy}} = 4.69$ (green), and $t/T_{\text{eddy}} = 6.25$ (red).

the best fit probability for every transition matrix element and then normalize rows, such that their summation is unity. The top graphs of Figure 8 display the best fit lines for the probability of the limbo state bin (for the lowest five initial bins), showing clearly that as particle radius increases, particle deposition becomes more likely at any bin. The best fit lines allows the probability of a transition matrix element to be estimated for any particle radius or diameter.

Once the transition matrix is inferred for a particle diameter of 35 μm, the random walk model is used to estimate the evolution of the vertical concentration profile under the same forcing conditions as presented earlier. In order to speed up the convergence of Lagrangian statistics, we set $\phi_s = 600/s$. The injection function ψ_I for the 35 μm particles is obtained from the LES and used as the input parameter in the upscaled model. For both the neutral and unstable boundary layers, the Markov chain model accurately captures the LES behavior shown in the bottom panels of Figure 8. Here our simple interpolation method provides robust results, suggesting that the dependence of the transition matrix on particle can be approximated, restricting the need for full LES runs to only a subset of particle size. Additionally, the predictions demonstrate that the difference in ϕ_s has little to no effect, suggesting that the particle statistics have converged.

4.2 Comparison to a 1-D analytical model

In this section we compare a previously-developed, 1-D analytical model with the LES results, in an effort to highlight the advantages of the proposed model. Specifically, we replicate vertical concentration profiles from the work of N18. In their model, the vertical gradient of mean concentration is calculated from the advection-diffusion equation

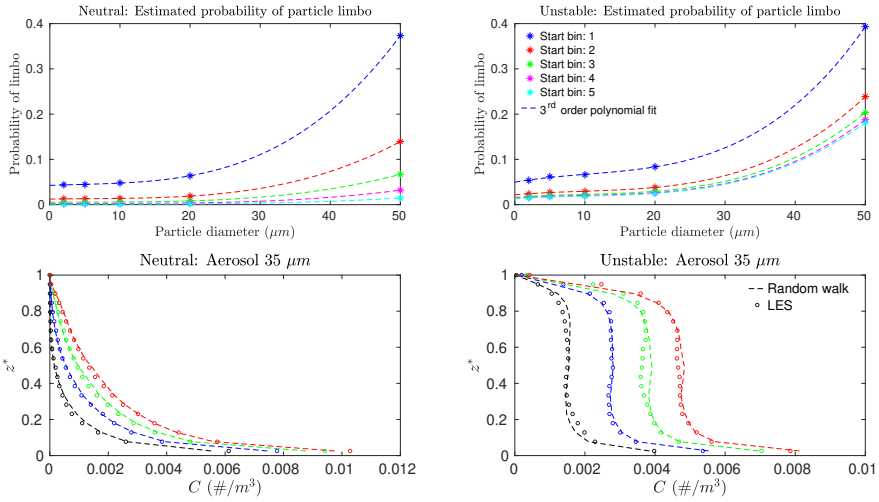

Figure 8. The top row shows the particle radius vs probability of limbo state and a best fit 3$^{\text{rd}}$-order polynomial for different atmospheric bins. The best fit polynomial is used to infer the transition matrix with diameter 35 μm. A transition matrix for an aerosol particle with a 35 μm diameter is inferred from transition matrices with other particle diameters. The temporal evolution of the concentration profiles from Markov chain model predictions (dashed lines) are compared with LES (dots) for the neutral (left) and unstable (right) cases. The temporal evolution is shown in the neutral case for $t/T_{\text{neut}} = 1$ (black), 2 (blue), 3 (green) and 4 (red). For the unstable case the data correspond to $t/T_{\text{eddy}} = 1.56$ (black), 3.13 (blue), 4.69 (green) and $= 6.25$ (red).

for a passive scalar with a constant settling velocity, under the assumptions of horizontal homogeneity, negligible molecular diffusivity, zero mean vertical velocity, turbulent vertical flux parameterized with an eddy-diffusivity, and a total (turbulent plus settling) vertical flux that decreases linearly with height from a constant surface flux Φ to zero at z_i. The final equation can be written as

$$\frac{dC}{dz} = -\frac{1}{K_c(z)}[w_s C + \Phi(1 - z/z_i)] \tag{8}$$

where C is the mean concentration and $K_c(z)$ is the eddy diffusivity.

In addition to the physical parameters that are constant in the simulation (u_*, z_i, w_s, Φ, and the Obukhov length L), equation (8) requires a model for the eddy diffusivity $K_c(z)$, proposed by N18 as

$$K_c(z) = \begin{cases} \dfrac{\kappa u_* z}{\phi(\zeta)}, & \text{if } z < 0.1 z_b, \\ a\dfrac{\kappa u_* z}{\phi(\zeta)}\left(1 - \dfrac{z}{z_i}\right)^2, & \text{if } z \geq 0.1 z_i, \end{cases} \tag{9}$$

where κ is the Von Kármán constant and $\phi(\zeta)$ is the stability function for a passive scalar in the surface layer ($\zeta = z/L$). This model extends the Monin-Obukhov similarity theory from the surface layer (Freire et al., 2016) to the entire ABL, through the use of a transitioning constant $a = 1/(1 - 0.1 z_i/z_i)^2$.

Figure 9 shows the comparison between N18's model and the LES results for the same cases evaluated with the Markov chain random walk model. Although no explicit

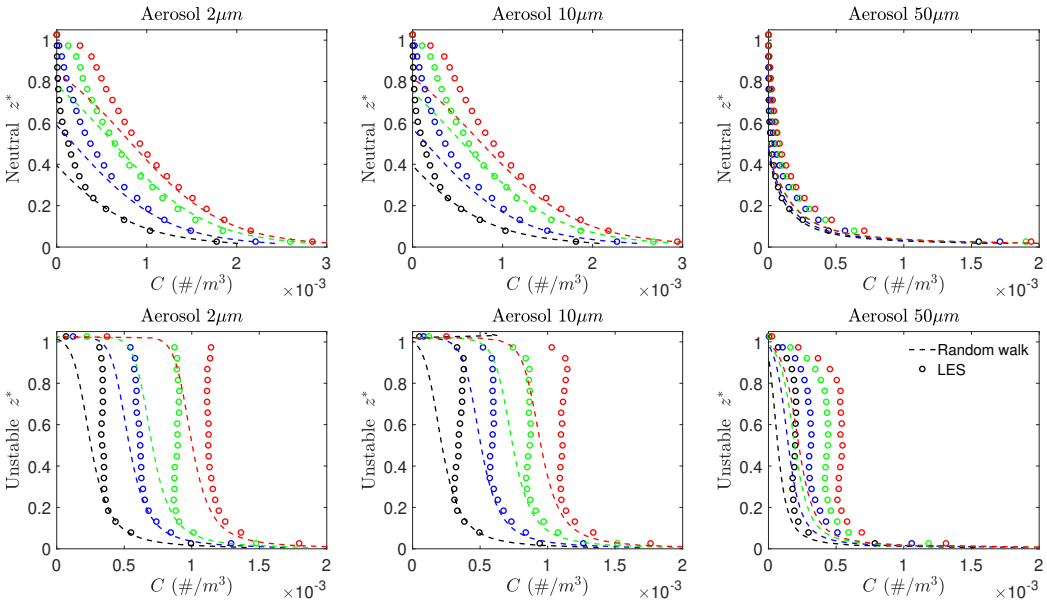

Figure 9. The temporal evolution of the vertical aerosol particle concentration profiles in the both neutral and unstable conditions for LES (dots) and 1-D analytical model proposed by Nissanka et al. (2018) (dashed lines) for particles with diameter $d = 2, 10, 50\,\mu$m for $T/T_{\text{neut}} = 0.25$ and $T/T_{\text{eddy}} = 1.56$ observation windows. The model time step is $T = 500\,$s for the neutral condition, and $T = 2000\,$s for the unstable condition. Colors correspond to $t/T_{\text{neut}} = 1.0$ and $t/T_{\text{eddy}} = 1.56$ (black), $t/T_{\text{neut}} = 2.0$ and $t/T_{\text{eddy}} = 3.13$ (blue), $t/T_{\text{neut}} = 3.0$ and $t/T_{\text{eddy}} = 4.69$ (green), $t/T_{\text{neut}} = 4.0$ and $t/T_{\text{eddy}} = 6.25$ (red).

time is shown in equation 8, the analytical solution varies in time because the reference concentration C_r (taken here as the surface concentration) changes in time: the theory assumes that the vertical profile is self-similar in its relationship between flux, surface concentration, and $C(z)$.

In both neutral and unstable cases, the analytical model matches the simulation at the surface layer for particles with diameters of 2 and 10 μm. For the 50 μm case, physical processes that are not taken into account by the analytical model (such as the trajectory-crossing effect) start to be relevant, and the model is not expected to work (Csanady, 1963; Freire et al., 2016). In addition, the behavior at the upper part of the atmosphere is likely affected by the strong inversion and the accumulation of particles, which is also not considered in the theoretical model. Finally, as noted by N18, the well-mixed behavior of the unstable cases cannot be well represented by an eddy-diffusivity approach (Stull, 1988; Wyngaard, 2010).

The random walk model is not constrained by the same assumptions, and can easily adapt to different conditions, as long as they are embedded in the estimation of the transition matrix M and an accurate representation of ψ_I. The critical case of well-mixed conditions is a clear example of this flexibility. The analytical model, on the other hand, is currently limited by the gradient diffusion approach to the turbulent transport parameterization. In addition, it does not consider the transient period of which aerosol particle growth in the MABL, as explained in N18. Thus, this new approach has the potential to go beyond the limitations of the 1-D analytical model, making it worth the pursuit of parameterizations for M and ψ_I.

4.3 The use of 1-D analytical models as ψ_I for the neutral boundary layer

In the previous analyses, we used LES to parameterize the Markov chain random walk model inputs, M and ψ_I. Here, we demonstrate that a theoretically-derived surface layer profile can instead be used for the injection initial condition ψ_I in the neutral ABL case. We use the model provided by Kind (1992) (hereafter referred to as K92), which corresponds to the mean concentration profile in the atmospheric surface layer (ASL) under steady-state and horizontally-homogeneous conditions:

$$\frac{C}{C_r} = \left(\frac{\Phi}{C_r w_s} + 1\right)\left(\frac{z}{z_r}\right)^{-\gamma} - \left(\frac{\Phi}{C_r w_s}\right), \tag{10}$$

where C is again the horizontal mean concentration, C_r is the reference concentration at the reference height z_r, Φ is the net concentration flux at the surface, and $\gamma = \tau_p g/\kappa u_*$ is the Rouse number (Rouse, 1937).

As shown in Figure 2, nearly all of the concentration remains within the surface layer ($z \leq 0.1 z_i$) for a time interval of $T/T_{neut} = 0.25$, a situation that allows the application of an ASL model such as K92's equation as an initial condition to the Markov chain random walk model. In this calculation, performed for $T/T_{\text{neut}} = 0.25$, the transition matrix used is the same as in previous analysis for the neutral ABL (section 3.1.2).

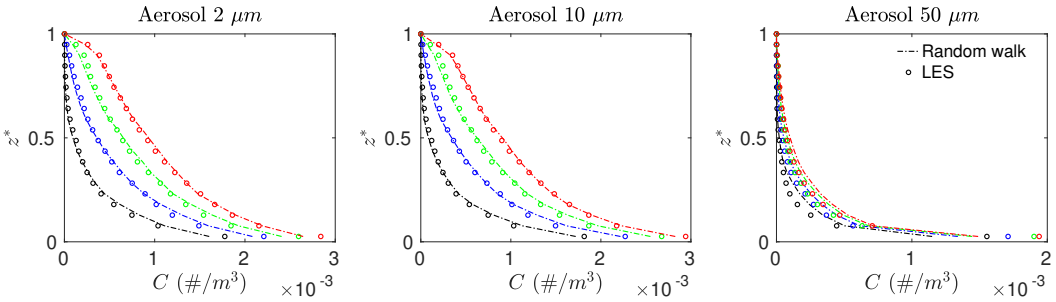

Figure 10. The temporal evolution of the vertical aerosol particle concentration profiles in the neutral case for the LES (dots), and using ψ_I based on Kind (1992) with the random walk model (dashed lines) for particles with diameter $d = 2, 10, 50\,\mu$m. Colors correspond to $t/T_{\text{neut}} = 1$ (black), 2 (blue), 3 (green), and 4 (red).

In Figure 10, concentration profiles calculated from the LES are compared to the Markov chain random walk model with an injection initial condition retrieved by K92's analytical model. The use of the theoretical profile as ψ_I in the neutral boundary layer continues to provide accurate predictions when comparing to the LES, especially for the $2\,\mu$m and $10\,\mu$m particle sizes. There exists a significant loss in predictive accuracy using the analytical model for $50\,\mu$m particles where the ASL model struggles, resulting in overprediction at nearly all heights.

Thus, it is clearly important for the initial injection condition ψ_I to be representative of the distribution of continually-sourced aerosol particles. If ψ_I does not capture the general particle transport features of the boundary layer, the predictions of the random walk model will have large errors even if M is perfect. As shown in Figure 9, in the unstable case the theoretical profiles have low accuracy above the surface layer, causing corresponding large errors in the random walk results if used as ψ_I (not shown). Additionally, the use of $T/T_{\text{eddy}} = 0.39$ causes an even larger mismatch for the 1-D analytical model prediction for the unstable case. As mentioned in N18, the initial transient

period is not taken into consideration, it will not accurately predict the aerosol particle growth in the boundary layer until these deficiencies are mitigated.

4.4 Upscaled model sensitivity and limitations

In this study, $T/T_{\text{neut}} = 0.25$ for the neutral case and two model time steps for the unstable case, $T/T_{\text{eddy}} = 0.39$ and $T/T_{\text{eddy}} = 1.56$, were demonstrated to accurately predict transport behavior. When $T \to 0$, particles do not have sufficient time for transport to other atmospheric height classes, meaning the transition matrix would have values of 1 along the diagonal and zero otherwise; clearly such a large positional correlation structure would not accurately predict particle transport. When T becomes much greater than the largest characteristic timescales of the flow, particle transport over successive steps becomes increasingly decorrelated (as observed in the unstable case with $T/T_{\text{eddy}} = 1.56$), and assuming independence over successive model steps becomes more valid. This removes the necessity of the Markov chain, represented by the transition matrix M. As $T \to \infty$, all particles hit the ocean surface and are removed from the system, while being replaced by particles in the same location according to ψ_I.

The sensitivity in predicted concentration profiles based on changes to the transition matrix remains an open question, and in this section our goal is to test this sensitivity in order to ensure that the model performance is robust. Additionally, this information can provide insight for a baseline parameterization for M. To do this, we run the random walk model with transition matrices whose elements have been artificially manipulated.

For the neutral case in Section 3.1.2, the transition matrix exhibited strong diagonal trending. Therefore, we adjust the probability that a particle remains in its current height class (i.e. the diagonal elements of the transition matrix) to 0, 50, and 150% of its actual value. Once the diagonal elements are adjusted, each row is normalized so its sum is unity.

In Figure 11, the temporal evolution of the concentration profiles is displayed for the random walk model whose transition matrices have been artificially adjusted. The ψ_I profile remains the same as the analysis done in Section 3.1.2. For all adjustments in the transition bins, the 10 μm diameter vertical profiles maintain an accurate prediction compared to the LES simulations. With no likelihood that a particle stays at the same height (left figures), and also for that with a higher probability (right figures), the random walk model loses little accuracy in the prediction of concentration profiles. Slight overprediction occurs at later time-steps in regions of large concentration (i.e. the surface layer), whereas in regions of lower concentrations (i.e. the inversion layer), the model underpredicts. Therefore, the Markov chain random walk model demonstrates a level of robustness based on the biased training of the transition matrix.

For testing the sensitivity in the unstable stratification case, we perform a different manipulation of the transition matrix. Knowing that the transition matrix is decorrelated when $T/T_{\text{eddy}} = 1.56$, (except at the inversion and surface deposition shown in Figure 7), we create a uniform transition matrix (top row of Fig. 12).

In Figure 12, the temporal evolution of the concentration profiles are presented for the modified transition matrices in the unstable case. Removal of the unstable correlation structure of the transition matrix affects the predictions at the top of the MABL, as concentrations become slightly over predicted. However, the profiles, as a whole, maintain accurate predictions in time, and again the random walk model appears robust to modifications of the transition matrix. As a result, a baseline for the parameterization of M can be used as a uniform matrix for the unstable case, with only a slight loss in accuracy at the inversion layer.

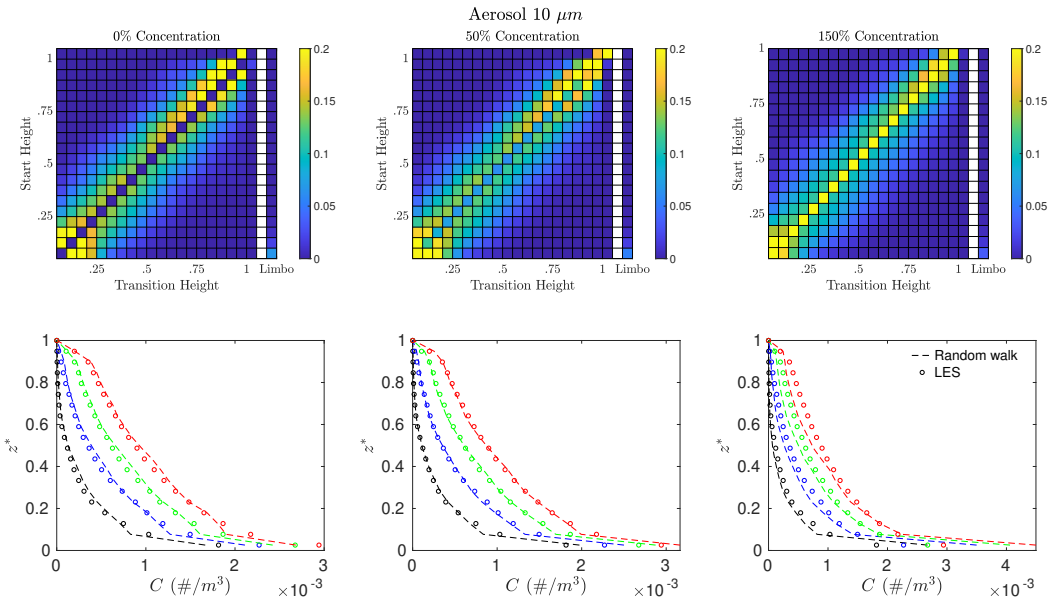

Figure 11. The temporal evolution of the vertical aerosol particle concentration profiles in neutral conditions for $d = 10\mu m$. Associated transition matrices are shown above for adjusted diagonal probabilities of 0%, 50%, and 150%. The incremental t/T_{eddy} are the same as in Figure 3.

5 Conclusions

In the present study we model the evolution of vertical aerosol particle concentrations for unstable and neutral boundary layer conditions over a range of particle sizes. To do so we introduce an upscaled random walk model, and LES is used as a testbed for comparison and informing upscaled model parameters. In order to accurately predict transport behavior, the boundary conditions and the physical processes that govern transport must be effectively upscaled. All of the physical processes related to vertical transport of aerosols considered by the LES are captured in a Markov chain random walk model. The benefit of this approach is that once parameterized, the proposed model is orders of magnitude more computationally efficient compared with LES modeling. The proposed Markov chain random walk model for one model time step T has a total run time of $O(0.01)$ cpu hours, while an LES runtime consists of roughly $O(10,000)$ cpu hours.

In the proposed framework, particles vertically transition through the MABL by random walk, which is enforced with a position correlation transition matrix. Hence, particle trajectories are modeled as a temporal Markov process. We test the upscaled model robustness by predicting the evolution of vertical concentration profiles for varying stability conditions and particle diameters. For all cases, the upscaled model faithfully represents transport behavior observed in the high fidelity LES. In comparison, 1-D analytical models cannot take into account the transient growth of the MABL's growth of aerosol particles, and also cannot obtain near-vertical concentrations in an unstable stratification environment. We demonstrate that for the neutral case, 1-D analytical models can be used to parameterize the injection initial condition ψ_I of our proposed upscaled model without degrading prediction accuracy. Finally the model, namely the transition matrix, is manipulated to explore it's sensitivity and limitations. This information provides a basis for parameterization for M.

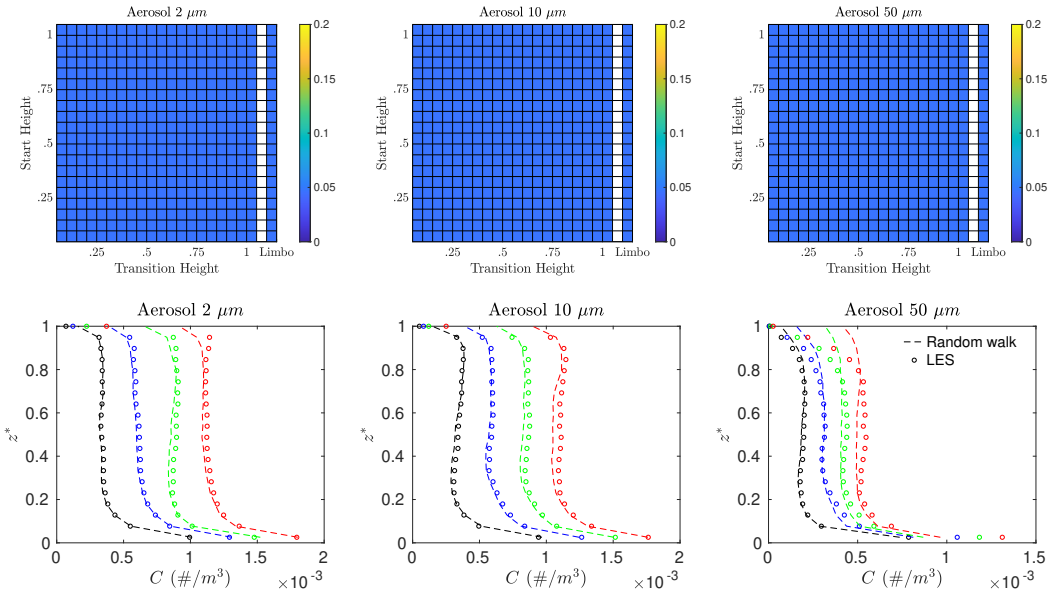

Figure 12. The temporal evolution of the vertical aerosol particle concentration profiles in an unstable stratification for a uniform transition matrix. The times t/T_{eddy} are the same as in Figure 7.

An outstanding challenge to the proposed modeling framework is the parameterization of the transition matrix without using LES. Currently, a major problem is that in order to predict transport behavior, transport first must be simulated. This has been a common problem in the subsurface hydrology community. However, recent advances have been made in analytic Markov models (Kang et al., 2015; Morales et al., 2017), inverse modeling approaches (Sherman et al., 2017, 2018), and assuming that correlation structures are governed by well known stochastic processes, such as Bernoulli or Ornstein-Uhlenbeck (Dentz et al., 2016; Hyman et al., 2019; Sherman et al., 2020). We envision that with some future effort similar methodologies may be applied in the context of the proposed MABL model and that our work here lays the ground motivating such advances.

Furthermore, the designation of T in the training of the transition matrix is still somewhat arbitrary, only as long as temporal stationarity is satisfied. In this study, the normalized random walk time step $T/T_{\text{neut}} = 0.25$ ($T = 500$s) for the neutral condition showed strong particle transport correlation, a feature well captured by the transition matrix. For the unstable boundary layer, the use of $T/T_{\text{eddy}} = 0.39$ showed weaker correlation, attributed by the large-scale convective structures of turbulence. Increasing the normalized model time step to $T/T_{\text{eddy}} = 1.56$ shows that the transition matrix is effectively decorrelated past the time-scale of one large scale eddy life cycle, relaxing the necessity of the Markov chain to the random walk model for model prediction. Once specific T are addressed, the upscaled Markov random walk may serve as a computationally efficient subgrid model that can be implemented in current boundary layer representation in global aerosol models.

Acknowledgments

HP, GW, and DR were supported by the Office of Naval Research (ONR) under Grant No. N00014-16-1-2472 and the National Science Foundation (NSF) under Grant No. AGS-1429921. LF was funded by São Paulo Research Foundation (FAPESP, Brazil) Grant

No. 2018/24284-1. Computational resources were provided by the Notre Dame Center for Research Computing. TS is supported by the National Science Foundation Graduate Research Fellowship under Grant No. DGE-1841556. Author JSR's contributions were supported by the Office of Naval Research Code 322 and the NRL Base Program. Data presented in this work can be found at: https://doi.org/10.5281/zenodo.3703180

References

Andreas, E. L. (1998). A new spray generation function for wind speeds up to 32 m/s. *Journal of Physical Oceanography*, *28*(11), 10. doi: 10.1175/1520-0485(1998)028⟨2175:ANSSGF⟩2.0.CO;2

Balachandar, S., & Eaton, J. K. (2010). Turbulent dispersed multiphase flow. *Annual Review of Fluid Mechanics*, *42*(1), 111–133. doi: 10.1146/annurev.fluid.010908.165243

Berkowitz, B., Cortis, A., Dentz, M., & Scher, H. (2006). Modeling non-fickian transport in geological formations as a continuous time random walk. *Reviews of Geophysics*, *44*(2). doi: 10.1029/2005RG000178

Bian, H., Froyd, K., Murphy, D. M., Dibb, J., Chin, M., Colarco, P. R., ... Smirnov, A. (2019). Observationally constrained analysis of sea salt aerosol in the marine atmosphere. *Atmospheric Chemistry and Physics Discussions*, 1–36. doi: 10.5194/acp-19-10773-2019

Blanchard, D. C., Woodcock, A. H., & Cipriano, R. J. (1984). The vertical distribution of the concentration of sea salt in the marine atmosphere near Hawaii. *Tellus B*, *36 B*(2), 118–125. doi: 10.1111/j.1600-0889.1984.tb00233.x

Bolster, D., Méheust, Y., Le Borgne, T., Bouquain, J., & Davy, P. (2014). Modeling preasymptotic transport in flows with significant inertial and trapping effects–the importance of velocity correlations and a spatial markov model. *Advances in water resources*, *70*, 89–103. doi: 10.1016/j.advwatres.2014.04.014

Brennen, C. E. (2005). *Fundamentals of multiphase flow*. Cambridge University Press.

Chamecki, M., Hout, R., Meneveau, C., & Parlange, M. B. (2007). Concentration profiles of particles settling in the neutral and stratified atmospheric boundary layer. *Boundary-Layer Meteorology*, *125*(1), 25–38. doi: 10.1007/s10546-007-9194-5

Christensen, J. H., Brandt, J., Frohn, L. M., & Skov, H. (2003). Modelling of mercury with the Danish Eulerian Hemispheric Model. *Atmospheric Chemistry and Physics Discussions*, *3*(4), 3525–3541.

Clarke, A. D., Owens, S. R., & Zhou, J. (2006). An ultrafine sea-salt flux from breaking waves: Implications for cloud condensation nuclei in the remote marine atmosphere. *Journal of Geophysical Research Atmospheres*, *111*(6), 1–14. doi: 10.1029/2005JD006565

Csanady, G. T. (1963). Turbulent diffusion of heavy particles in the atmosphere. *Journal of the Atmospheric Sciences*, *20*(3), 201–208. doi: 10.1175/1520-0469(1963)020⟨0201:TDOHPI⟩2.0.CO;2

De Anna, P., Le Borgne, T., Dentz, M., Tartakovsky, A. M., Bolster, D., & Davy, P. (2013). Flow intermittency, dispersion, and correlated continuous time random walks in porous media. *Physical review letters*, *110*(18), 184502. doi: 10.1103/PhysRevLett.110.184502

Deardorff, J. W. (1972). Numerical investigation of neutral and unstable planetary boundary layers. *Journal of the Atmospheric Sciences*, *29*, 91–115. doi: 10.1175/1520-0469(1972)029⟨0091:NIONAU⟩2.0.CO;2

Deardorff, J. W. (1980). Stratocumulus-capped mixed layers derived from a three-dimensional model. *Boundary-Layer Meteorology*, *18*(4), 495–527. doi: 10.1007/BF00119502

Delay, F., Ackerer, P., & Danquigny, C. (2005). Simulating solute transport in

porous or fractured formations using random walk particle tracking: A review. *Vadose Zone Journal*, *4*(2), 360–379. doi: 10.2136/vzj2004.0125

de Leeuw, G., Neele, F. P., Hill, M., Smith, M. H., & Vignati, E. (2000). Production of sea spray aerosol in the surf zone. *Journal of Geophysical Research*, *105*(D24), 29397. doi: 10.1029/2000JD900549

Dentz, M., Kang, P. K., Comolli, A., Le Borgne, T., & Lester, D. R. (2016). Continuous time random walks for the evolution of lagrangian velocities. *Physical Review Fluids*, *1*(7), 074004.

Erickson, D. J., Seuzaret, C., Keene, W. C., & Gong, S. L. (1999). A general circulation model based calculation of HCl and ClNO2 production from sea salt dechlorination: reactive chlorine emissions inventory. *Journal of Geophysical Research Atmospheres*, *104*(D7), 8347–8372. doi: 10.1029/98JD01384

Freire, L. S., Chamecki, M., & Gillies, J. A. (2016). Flux-profile relationship for dust concentration in the stratified atmospheric surface layer. *Boundary-Layer Meteorology*, *160*(2), 249–267. doi: 10.1007/s10546-016-0140-2

Gerber, H. (1991). Supersaturation and droplet spectral evolution in fog. *Journal of the Atmospheric Sciences*, *48*(24), 2569–2588. doi: 10.1175/1520-0469(1991)048⟨2569:SADSEI⟩2.0.CO;2

Ghan, S. J., Guzman, G., & Abdul-Razzak, H. (1998). Competition between sea salt and sulfate particles as cloud condensation nuclei. *Journal of the Atmospheric Sciences*, *55*(22), 3340–3347. doi: 10.1175/1520-0469(1998)055⟨3340:CBSSAS⟩2.0.CO;2

Giuggioli, L., Sevilla, F. J., & Kenkre, V. (2009). A generalized master equation approach to modelling anomalous transport in animal movement. *Journal of Physics A: Mathematical and Theoretical*, *42*(43), 434004. doi: 10.1088/1751-8113/42/43/434004

Hoppel, W. A., Frick, G. M., & Fitzgerald, J. W. (2002). Surface source function for sea-salt aerosol and aerosol dry deposition to the ocean surface. *Journal of Geophysical Research Atmospheres*, *107*(19), 1–17. doi: 10.1029/2001JD002014

Hyman, J., Dentz, M., Hagberg, A., & Kang, P. K. (2019). Linking structural and transport properties in three-dimensional fracture networks. *Journal of Geophysical Research: Solid Earth*, *124*(2), 1185–1204.

Kang, P. K., Le Borgne, T., Dentz, M., Bour, O., & Juanes, R. (2015). Impact of velocity correlation and distribution on transport in fractured media: Field evidence and theoretical model. *Water Resources Research*, *51*(2), 940–959. doi: 10.1002/2014WR015799

Kind, R. J. (1992). One-dimensional aeolian suspension above beds of loose particles-A new concentration-profile equation. *Atmospheric Environment Part A, General Topics*, *26*(5), 927–931. doi: 10.1016/0960-1686(92)90250-O

Klemp, J. B., & Durran, D. R. (1983). An Upper Boundary Condition Permitting Internal Gravity Wave Radiation in Numerical Mesoscale Models. *Monthly Weather Review*, *111*(3), 430–444. doi: 10.1175/1520-0493(1983)111⟨0430:aubcpi⟩2.0.co;2

Lamb, R. G. (1978). A numerical simulation of dispersion from an elevated point source in the convective planetary boundary layer. *Atmospheric Environment*, *12*(6-7), 1297–1304. doi: 10.1016/0004-6981(78)90068-9

Le Borgne, T., Dentz, M., & Carrera, J. (2008). Lagrangian statistical model for transport in highly heterogeneous velocity fields. *Physical review letters*, *101*(9), 090601. doi: 10.1103/PhysRevLett.101.090601

Lewis, E. R., & Schwartz, S. E. (2004). *Sea salt aerosol production: mechanisms, methods, measurements, and models-a critical review*. Washington, DC, American Geophysical Union.

Moeng, C.-H. (1984). A large-eddy-simulation model for the study of planetary boundary-layer turbulence. *Journal of the Atmospheric Sciences*, *41*(13),

2052–2062. doi: 10.1175/1520-0469(1984)041⟨2052:ALESMF⟩2.0.CO;2

Moeng, C.-H., & Sullivan, P. P. (1994). A comparison of shear- and buoyancy-driven planetary boundary layer flows. *Journal of the Atmospheric Sciences*, *51*(7), 999–1022. doi: 10.1175/1520-0469(1994)051⟨0999:ACOSAB⟩2.0.CO;2

Montero, M., & Masoliver, J. (2017). Continuous time random walks with memory and financial distributions. *The European Physical Journal B*, *90*(11), 207. doi: 10.1140/epjb/e2017-80259-4

Morales, V. L., Dentz, M., Willmann, M., & Holzner, M. (2017). Stochastic dynamics of intermittent pore-scale particle motion in three-dimensional porous media: Experiments and theory. *Geophysical Research Letters*, *44*(18), 9361–9371. doi: 10.1002/2017GL074326

Nelson, J. (1999). Continuous-time random-walk model of electron transport in nanocrystalline tio 2 electrodes. *Physical Review B*, *59*(23), 15374. doi: 10.1103/PhysRevB.59.15374

Nissanka, I. D., Park, H. J., Freire, L. S., Chamecki, M., Reid, J. S., & Richter, D. H. (2018). Parameterized vertical concentration profiles for aerosols in the marine atmospheric boundary layer. *Journal of Geophysical Research: Atmospheres*, *123*(17), 9688–9702. doi: 10.1029/2018JD028820

Peng, T., & Richter, D. (2019). Sea spray and its feedback effects: Assessing bulk algorithms of air-sea heat fluxes via direct numerical simulations. *Journal of Physical Oceanography*, *49*(6), 1403–1421. doi: 10.1175/JPO-D-18-0193.1

Prandtl, L. (1981). *Essentials of fluid dynamics*. Blackie and Son, London.

Quinn, P. K., Collins, D. B., Grassian, V. H., Prather, K. A., & Bates, T. S. (2015). Chemistry and related properties of freshly emitted sea spray aerosol. *Chemical Reviews*, *115*(10), 4383–4399. doi: 10.1021/cr500713g

Reid, J. S., Jonsson, H. H., Smith, M. H., & Smirnov, A. (2001). Evolution of the vertical profile and flux of large sea-salt particles in a coastal zone. *Journal of Geophysical Research Atmospheres*, *106*(D11), 12039–12053. doi: 10.1029/2000JD900848

Reid, J. S., Reid, E. A., Walker, A., Piketh, S., Cliff, S., Mandoos, A. A., ... Eck, T. F. (2008). Dynamics of southwest Asian dust particle size characteristics with implications for global dust research. *Journal of Geophysical Research Atmospheres*, *113*(14), 1–14.

Richter, D. H., Dempsey, A. E., & Sullivan, P. P. (2019). Turbulent transport of spray droplets in the vicinity of moving surface waves. *Journal of Physical Oceanography*, *49*(7), 1789–1807. doi: 10.1175/JPO-D-19-0003.1

Riemer, N., Vogel, H., Vogel, B., & Fiedler, F. (2003). Modeling aerosols on the mesoscale-γ: Treatment of soot aerosol and its radiative effects. *Journal of Geophysical Research D: Atmospheres*, *108*(19). doi: 10.1029/2003JD003448

Rouse, H. (1937). Modern conceptions of the mechanics of fluid turbulence. *American Society of Civil Engineers Transactions*, *102*.

Scalas, E. (2006). The application of continuous-time random walks in finance and economics. *Physica A: Statistical Mechanics and its Applications*, *362*(2), 225–239. doi: 10.1016/j.physa.2005.11.024

Sherman, T., Fakhari, A., Miller, S., Singha, K., & Bolster, D. (2017). Parameterizing the Spatial Markov Model From Breakthrough Curve Data Alone. *Water Resources Research*, *53*(12), 10888–10898. doi: 10.1002/2017WR021810

Sherman, T., Foster, A., Bolster, D., & Singha, K. (2018). Predicting downstream concentration histories from upstream data in column experiments. *Water Resources Research*, *54*(11), 9684–9694. doi: 10.1029/2018WR023420

Sherman, T., Hyman, J., Dentz, M., & Bolster, D. (2020). Characterizing the influence of fracture density on network scale transport. *Journal of Geophysical Research: Solid Earth*.

Sherman, T., Roche, K. R., Richter, D. H., Packman, A. I., & Bolster, D. (2019). A dual domain stochastic lagrangian model for predicting transport in open

channels with hyporheic exchange. *Advances in water resources*, *125*, 57–67. doi: 10.1016/j.advwatres.2019.01.007

Stolaki, S., Haeffelin, M., Lac, C., Dupont, J. C., Elias, T., & Masson, V. (2015). Influence of aerosols on the life cycle of a radiation fog event. A numerical and observational study. *Atmospheric Research*, *151*, 146–161. doi: 10.1016/j.atmosres.2014.04.013

Stull, R. (1988). *An introduction to boundary layer meteorology.* Springer Netherlands.

Sullivan, P. P., & Patton, E. G. (2011). The effect of mesh resolution on convective boundary layer statistics and structures generated by large-eddy simulation. *Journal of the Atmospheric Sciences*, *68*(10), 2395–2415. doi: 10.1175/JAS-D-10-05010.1

Sund, N. L., Bolster, D., & Dawson, C. (2015). Upscaling transport of a reacting solute through a peridocially converging-diverging channel at preasymptotic times. *Journal of Contaminant Hydrology*, *182*, 1–15. doi: 10.1016/j.jconhyd.2015.08.003

Toba, Y. (1965). On the giant sea-salt particles in the atmosphere I. General features of the distribution. *Tellus*, *17*(1), 131–145. doi: 10.3402/tellusa.v17i1.8997

Van Kampen, N. (1979). Composite stochastic processes. *Physica A: Statistical Mechanics and its Applications*, *96*(3), 435–453.

Veron, F. (2015). Ocean spray. *Annual Review of Fluid Mechanics*, *47*, 507–538. doi: 10.1146/annurev-fluid-010814-014651

Winkler, P. (1988). The growth of atmospheric aerosol particles with relative humidity. *Physica Scripta*, *37*(2), 223–230. doi: 10.1088/0031-8949/37/2/008

Wyngaard, J. C. (2010). *Turbulence in the atmosphere.* Cambridge University Press.

Wyngaard, J. C., & Brost, R. A. (1984). Top-down and bottom-up diffusion of a scalar in the convective boundary layer. *Journal of the Atmospheric Sciences*, *41*(1), 102–112. doi: 10.1175/1520-0469(1984)041⟨0102:TDABUD⟩2.0.CO;2